33rd Annual International Conference of the IEEE EMBS
Boston, Massachusetts USA, August 30 - September 3, 2011

Predicting the Optimal Position and Direction of a Ubiquitous ECG using a Multi-Scale Model of Cardiac Electrophysiology

Ki Moo Lim, Seong Bae Hong, Jae Won Jeon, Min Su Gyung, Byung Hoon Ko, Sang Kon Bae, Kun Soo Shin, and Eun Bo Shim, *Member, IEEE*

***Abstract*—In this study, we determined the optimal position and direction of a one-channel bipolar electrocardiogram (ECG), used ubiquitously in healthcare. To do this, we developed a three-dimensional (3D) electrophysiological model of the heart coupled with a torso model that can generate a virtual body surface potential map (BSPM). Finite element models of the atria and ventricles incorporated the electrophysiological dynamics of atrial and ventricular myocytes, respectively. The torso model, in which the electric wave pattern on the cardiac tissue is reflected onto the body surface, was implemented using a boundary element method. Using the model, we derived the optimal positions of two electrodes, 5 cm apart, of the bipolar ubiquitous ECG (U-ECG) for detecting the P, R, and T waves. This model can be used as a simulation tool to design U-ECG device for use for various arrhythmia and normal patients.**

I. Introduction

As the era of ubiquitous healthcare begins, many conventional medical devices are redesigned for ubiquitous healthcare purposes. One of the examples is ubiquitous ECG on which many researches are conducted. Recently, a bipolar mini-ECG (U-ECG) for ubiquitous healthcare has been introduced and various studies about the U-ECG are in progress [1, 2]. The U-ECG is a small patch-shaped device with two electrodes. It is easily attachable on torso surface and can be utilized for ubiquitous healthcare since it is capable of wireless transmission. However, since it has two electrodes in a small area of the torso surface, it requires an optimal design suitable for detecting ECG signals. Especially, the position and direction of the device on the torso surface and the distance between electrodes are essential design parameters that determine the quality of device performance. In order to determine these design parameters, a detailed data of potential distribution on torso surface is required. Measuring device of body surface potential map (BSPM) can be used to get the data, but it is difficult to obtain a data with spatially enough resolution due to noise or limited number of electric sensors on torso.

A computational method can be used as an alternative. Since this method is cost-effective and can quickly provide solution, it is widely used in optimal design of medical devices. However, no computational analysis of the BSPM has been used to design the U-ECG. Several research groups have constructed electrophysiological models of the atria and ventricles [3, 4], and some research generated a pseudo-BSPM using an electrophysiological model of the heart coupled with a torso model [5-7]. Previously, we developed a three-dimensional (3D) finite element (FE) model of the human ventricles, coupled with a torso model, and generated a pseudo-BSPM to analyze ventricular tachycardia.

In this study, we developed a 3D electrophysiological model of the heart that incorporates both the atria and ventricles, by combining existing models of the human atria and ventricles. The heart model is coupled with an electrical model of a human torso to generate a pseudo-BSPM. Using this model, we determined the optimal position and direction of two U-ECG electrodes 5 cm apart for detecting the P, R, and T peaks.

II. Methods

To simulate electrical conduction in the human heart and torso, we developed a 3D-FE model of the human heart that incorporates an electrophysiological representation of cardiac myocytes, coupled with a boundary element (BE) model of the human torso surface. The human heart model includes an atrium model and a ventricle model. The atrium model we used was the human atrial cell model of Nygren *et al*. [8] based on the human atrium geometry of Harrild and Henriquez [9]. For

Following are results of a study on the "Human Resource Development Center for Economic Region Leading Industry" Project, supported by the Ministry of Education, Science & Technology (MEST) and the National Research Foundation of Korea (NRF) and have also been supported by Samsung Electronics.

Corresponding author: Eun Bo Shim is with the Department of Mechanical & Biomedical Engineering, Kangwon National University, Chuncheon, Ganwon-do, South Korea. (phone: 82-33-250-6318; e-mail: ebshim@kangwon.ac.kr; fax: 82-33-257-6595)

Ki Moo Lim is with the Department of Mechanical & Biomedical Engineering, Kangwon National University, Chuncheon, Ganwon-do, South Korea (kmlimphd@gmail.com).

Seong Bae Hong is with the Department of Mechanical & Biomedical Engineering, Kangwon National University, Chuncheon, Ganwon-do, South Korea (seungbae@kangwon.ac.kr).

Jae Won Jeon is with the Department of Mechanical & Biomedical Engineering, Kangwon National University, Chuncheon, Ganwon-do, South Korea (skyjaewon@gmail.com).

Min Su Gyung is with the Department of Mechanical & Biomedical Engineering, Kangwon National University, Chuncheon, Ganwon-do, South Korea (gyoun-woo@nate.com).

Byung Hoon Ko is with the Samsung Electronics, Yongin, Gyunggi-do, South Korea.

Sang Kon Bae is with the Samsung Electronics, Yongin, Gyunggi-do, South Korea.

Kun Soo Shin is with the Samsung Electronics, Yongin, Gyunggi-do, South Korea.

the ventricle model, the four-variable human ventricular cell model of Bueno-Orovio *et al*. [10] based on the canine ventricle geometry of Hunter *et al*. [4] was scaled to the size of the human ventricles. Then, the two-dimensional Purkinje network of Berenfeld and Jalife [11] was mapped onto the three-dimensional endocardial surface (Fig 1). In order to connect electrical propagation in atrium to ventricular tissue, we stimulated AV node at 100 ms (AV node delay) after the terminal of intermodal tract in atrium are excited.

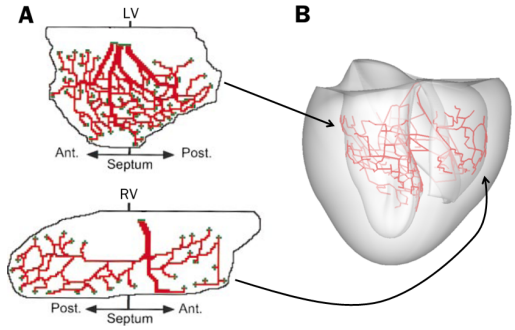

Fig. 1 A two dimensional (2D) representation of the left and right Purkinje network (A) and 3D ventricle model with the Purkinje newtwork mapped into 3D space. LV, left ventricle; RV, right ventricle; Post., posterior wall; Ant., anterior wall.

A. 3D FE Electrophysiological Model of the Human Heart

The human heart model incorporates a 3D atrial tissue model and a ventricular tissue model using the mono-domain method. The mono-domain model of the 3D heart can be described using the following partial differential equation for the reaction-diffusion form:

$$\frac{\partial V_m}{\partial t} = \nabla \cdot \left(D\left(\sigma_{mL}, \sigma_{mT}\right) \nabla V_m \right) - I_m \qquad (1)$$

where V_m is the membrane voltage, t is the time, D is the diffusion tensor of electric wave propagation, and σ_{mL} and σ_{mT} are the conductivities parallel and perpendicular to the fiber axis, respectively. I_m is the membrane current, which is formulated differently according to the cell type. I_m in an atrial cell is described by the following equation:

$$I_m = \frac{I_{Na} + I_{Ca,L} + I_t + I_{sus} + I_{K1} + I_{b,Na} + I_{b,Ca} + I_{NaK} + I_{CaP} + I_{NaCa} - I_{stim}}{C_m} \qquad (2)$$

I_m in a ventricular cell is described by the following equation:

$$I_m = J_{fi} + J_{so} J_{si} \qquad (3)$$

All of the parameters and variables in Equations 2 and 3 are outlined in Nygren *et al*. [8] and Bueno-Orovio *et al*. [10], respectively.

B. 3D BE Electrical Model of Human Torso

To map the electrical potential throughout the heart into the torso surface, the BE model of the human torso of Potse *et al*. was used [5]. The potential at the torso surface is described by the following equation:

$$\phi_{ek}(r) = \frac{1}{2\pi\left(\sigma_k^- + \sigma_k^+\right)} \cdot \left[\int J_c(r') \cdot \frac{r - r'^3}{|r - r'|^3} dV' + \sum_l \int_{Sl} \left(\sigma_l^- - \sigma_l^+\right) \phi_e(r'') d\Omega_{rr''} \right] \qquad (6)$$

where $\phi_{ek}(r)$ is potential at a point r on surface k. σ_k^- and σ_k^+ indicate the conductivity inside and outside surface k, respectively, J_c is the source current density field, and r' and r'' are variables. The summation is over all surfaces l. $d\Omega_{rr''}$ is the solid angle subtended at r by the infinitesimal surface element situated at r''. The model is described in more detail in Potse *et al*. [5].

C. Validation of the model.

To validate the virtual heart and torso model, we, first, reconstructed a cellular electrophysiological response of the atrium and ventricle that included epicardial, endocardial, and midmyocardial cells. Electric activation time maps for the atria and ventricle were generated for verifying electrical conduction pattern. Finally, virtual BSPM and standard 12 lead ECG waveforms were generated.

D. Amplitude Maps for the P, R, and T waves

Fig. 2a is a schematic diagram of the U-ECG device attached to the human torso surface. The U-ECG has three electrodes: the two electrodes at each end (Electrodes A and Electrode B in Fig. 2a) are bipolar electrodes, while the one in the middle is the ground electrode. The bipolar electrodes are 5 cm apart.

Using the time-varying pseudo-BSPM data obtained from the electrophysiological models of the heart and torso, we generated amplitude maps for the P, R, and T waves given a 5-cm distance between the two U-ECG electrodes. This map shows the direction of the U-ECG and the amplitude of the peaks. This is done using the following steps:

1) BSPM data are collected every millisecond for one cardiac cycle (0–800 ms). They are generated from the electrophysiological model of the human heart coupled with the torso model.
2) We generated the ECG wave by subtracting the potential at Electrode A, located on the torso surface, from that at Electrode B, located 5 cm distant on the torso (Fig. 2b).
3) Step 2 is repeated for all nodes on the torso surface.
4) From among the various waveforms corresponding to the specific position of Electrode A on the torso surface, we identified the ECG waveform with the highest amplitude of a specific wave (*i.e*., the P wave, QRS complex, or T wave) and the corresponding position of Electrode B.
5) Step 4 is repeated for all nodes on the torso surface.
6) Steps 1 to 5 are repeated to obtain the optimal position and direction of the 5-cm U-ECG for the P, QRS, and T waves individually.

III. RESULTS

Fig. 3 shows the action potential waveforms of an atrial cell and ventricular epicardial, endocardial, and midmyocardial

cells. The shapes of each action potential matched previous results [8, 10]. The action potential duration was 220, 269, 260, and 410 ms in the atrial, epicardial, endocardial, and midmyocardial cells, respectively.

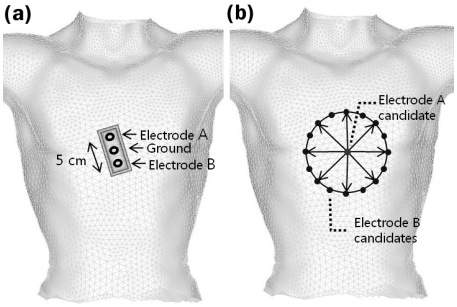

Fig. 2. Schematic of the U-ECG device attached to the torso surface (a) and a description of how to determine the optimal position and direction of the U-ECG (b).

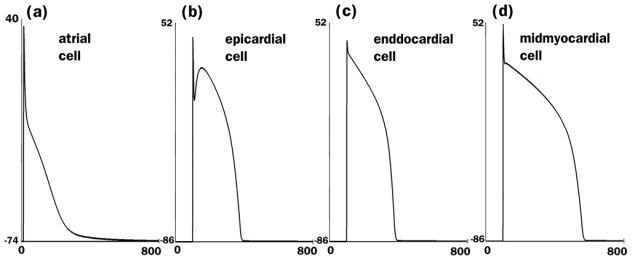

Fig. 3. Simulated action potential waves of atrial (a) and ventricular epicardial (b), endocardial (c), and midmyocardial (d) cells.

Fig. 4 shows the activation time maps for the atrium and ventricle. The electrical conduction pattern also matched previous results [6, 9]. For the atria, the electrical stimulation starts from the sinoatrial node beside the superior vena cava in the right atrium and ends at the base of the left atrium. For the ventricles, the electrical stimulation starts from the peripheral node of the Purkinje system in the left and right ventricular endocardium and ends at the base of the right ventricle.

Fig. 5 shows pseudo-BSPMs during P (50 ms), QRS (165 ms), and T (467 ms) waves. Two extrema (positive and negative) were generated as indicated by Trudel et al [6]. The difference between the potentials of two extrema (negative and positive) is most significant at t = 165 ms at which QRS complex was generated and least significant at t = 50 ms at which P wave was generated.

Fig. 6 shows the calculated 12-lead ECG waveforms. The R peak is highest in lead II. The width of the QRS complex was 80 ms, which is within the normal range. The P, QRS, and T waves were all reversed in aVR. A deep S wave was observed in V1, V2, and V3. The R peak was highest in V4 among the precordial leads. The 12 waveforms match clinical normal data well.

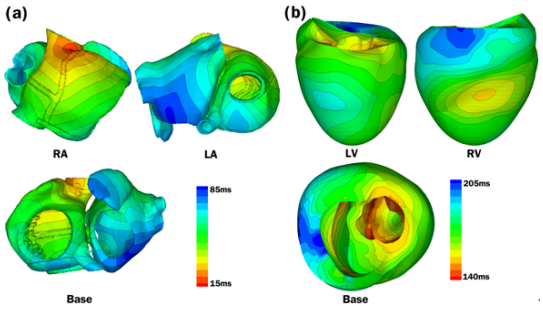

Fig. 4. Calculated activation time maps for the atria (A) and ventricles (B). RA, right atrium; LA, left atrium; LV, left ventricle; RV, right ventricle.

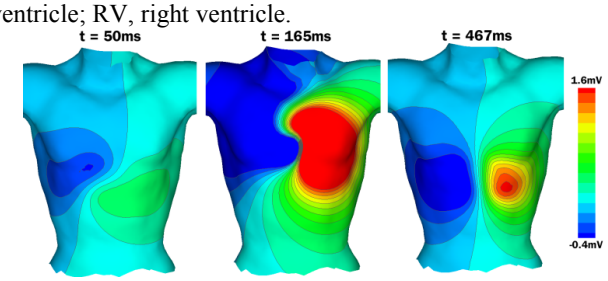

Fig. 5. Simulated isopotential maps of the torso when the P (left, t = 50 ms), R (middle, t = 165 ms), and T (right, t = 467 ms) peaks are generated.

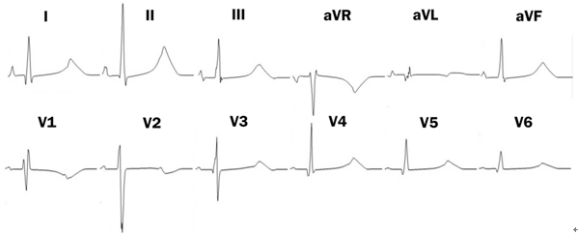

Fig. 6. ECG waveforms of the 12 standard leads.

Fig. 7 shows the amplitude maps and direction of the U-ECG for the P (a), QRS (b), and T (c) waves at the position where the highest amplitude is generated and corresponding lead ECG waveforms (d-f). For the P peak, the optimal position of the U-ECG is to the right and above the atrium and the direction is left and downwards. The corresponding ECG waveform demonstrated clear P wave despite equivocal QRS and T waves. For the R peak, the optimal position is to the right of atrioventricular node and the direction is leftward. The corresponding ECG waveform is . For the T peak, the optimal position is to the right of the ventricles and the direction is left. The optimal direction of the U-ECG is indicated with arrows.

IV. DISCUSSION AND CONCLUSIONS

The 12-lead ECG has been the standard clinical tool for assessing cardiac disease and can provide general information about cardiac electric activity. As a part of ubiquitous health care, various U-ECGs have been developed and studied by many research groups. However, most U-ECG research has

examined communications, data transmission, or signal processing. Few research groups have approached the design of the optimal U-ECG theoretically for detecting patient clinical information. In this study, we predicted the optimal position and direction of a U-ECG with electrodes 5 cm apart for detecting the P, R, and T peaks. To do this, we combined 3D FE electrophysiological models of the human atria and ventricles. The electrical activity from the entire heart was mapped onto a BE model of the human torso. This resulted in a pseudo-BSPM data, which included the effects of both the atria and ventricles.

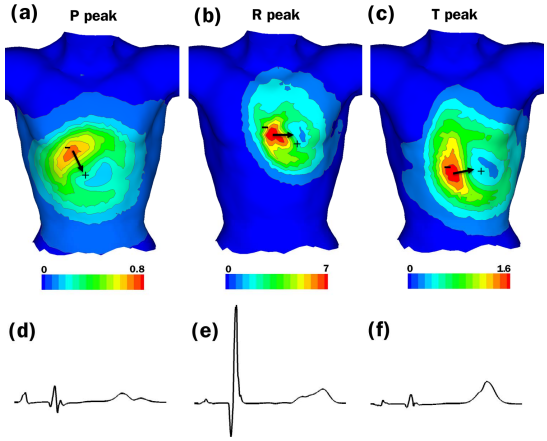

Fig. 7. Amplitude maps and positions of the U-ECG for the P (a), QRS (b), and T (c) waves. The start and end points of arrows indicate the optimal positions for the two electrodes of U-ECG to be attached. Corresponding lead ECG waveforms are shown in (d)-(f) and within normal limits.

At the cellular level, the action potential waveforms of the atria and ventricles (Fig. 3) matched experimental results well [8, 10]. At the organ level, the electrical conduction pattern (Fig. 4) also matched previous results well [6, 9]. The pseudo-BSPM (Fig. 5) and corresponding ECG waveforms (Fig. 6) were also within normal variation.

Amplitude maps and the directions of the U-ECG for detecting the P, QRS, and T waves were determined using our verified, integrated BSPM simulator. This model may be used as a simulation tool for designing U-ECGs to be used in patients with various arrhythmias, and in normal individuals.

Clinical implication. Electro-cardiological condition of heart failure or arrhythmia patients can be monitored for 24 hours by the U-ECG device to prevent sudden cardiac death. Various researches of the U-ECG to date are almost about signal processing of detected ECG signal or communication between sensor and monitoring user interface to obtain almost same signal as detected signal on the U-ECG patches. In addition to the researches, the determination of appropriate position for the U-ECG in this study will provide better source signal of ECG waveform. Therefore, this result will improve the quality of final ECG waveforms.

Limitation. We assumed that there is nothing between body surface and heart in the model. Though atria model is based on human atria geometry, ventricular model is based on the canine heart geometry. However, the size of the ventricle was scaled to the human heart size: this will not have much effect on ECG waveforms.

V. REFERENCES

[1] W. Shin, Y. D. Cha, and G. Yoon, "ECG/PPG integer signal processing for a ubiquitous health monitoring system," *J Med Syst,* vol. 34, p. 891-8, Oct. 2010.

[2] Y. D. Cha and G. Yoon, "Ubiquitous health monitoring system for multiple users using a ZigBee and WLAN dual-network," *Telemed J E Health,* vol. 15, p. 891-7, Nov. 2009.

[3] F. Vadakkumpadan, L. J. Rantner, B. Tice, P. Boyle, A. J. Prassl, E. Vigmond, . . . N. Trayanova, "Image-based models of cardiac structure with applications in arrhythmia and defibrillation studies," *J Electrocardiol,* vol. 42, p. 157 e1-10, Mar-Apr. 2009.

[4] P. J. Hunter, A. J. Pullan, and B. H. Smaill, "Modeling total heart function," *Annu Rev Biomed Eng,* vol. 5, p. 147-77, 2003.

[5] M. Potse, B. Dube, and A. Vinet, "Cardiac anisotropy in boundary-element models for the electrocardiogram," *Med Biol Eng Comput,* vol. 47, p. 719-29, Jul. 2009.

[6] M. C. Trudel, B. Dube, M. Potse, R. M. Gulrajani, and L. J. Leon, "Simulation of QRST integral maps with a membrane-based computer heart model employing parallel processing," *IEEE Trans Biomed Eng,* vol. 51, p. 1319-29, Aug. 2004.

[7] U. B. Im, S. S. Kwon, K. Kim, Y. H. Lee, Y. K. Park, C. H. Youn, and E. B. Shim, "Theoretical analysis of the magnetocardiographic pattern for reentry wave propagation in a three-dimensional human heart model," *Prog Biophys Mol Biol,* vol. 96, p. 339-56, Jan-Apr. 2008.

[8] A. Nygren, C. Fiset, L. Firek, J. W. Clark, D. S. Lindblad, R. B. Clark, and W. R. Giles, "Mathematical model of an adult human atrial cell: the role of K+ currents in repolarization," *Circ Res,* vol. 82, p. 63-81, Jan 9-23. 1998.

[9] D. Harrild and C. Henriquez, "A computer model of normal conduction in the human atria," *Circ Res,* vol. 87, p. E25-36, Sep 29. 2000.

[10] A. Bueno-Orovio, E. M. Cherry, and F. H. Fenton, "Minimal model for human ventricular action potentials in tissue," *J Theor Biol,* vol. 253, p. 544-60, Aug 7. 2008.

[11] O. Berenfeld and J. Jalife, "Purkinje-muscle reentry as a mechanism of polymorphic ventricular arrhythmias in a 3-dimensional model of the ventricles," *Circ Res,* vol. 82, p. 1063-77, Jun 1. 1998.